Electronic structure of nanometric Si/C, Si/N, and Si/C/N powders studied by both x-ray-photoelectron and soft-x-ray spectroscopies

M. Driss-Khodja, A. Gheorghiu, G. Dufour, H. Roulet, C. Sénémaud
Laboratoire de Chimie-Physique, URA CNRS 176, Université Pierre et Marie Curie, 11 Rue Pierre et Marie Curie, 75231 Paris Cedex 05, France

M. Cauchetier
S.P.A.M. Bâtim 522, CE Saclay, 91191 Gif-s-Yvette, France
(Received 10 April 1995; revised manuscript received 2 August 1995)

The electronic structure of nanometric Si/C, Si/N, and Si/C/N powders prepared by laser synthesis from appropriate gas mixtures has been investigated by using two complementary experimental methods. The total and partial Si $3p$ valence-band (VB) distributions were obtained from X-ray-photoelectron and soft-x-ray-emission spectra, respectively; the conduction-band (CB) Si p states were studied through the Si K x-ray-photoabsorption spectrum. For the binary compounds, the results confirm that the laser-synthesized (LS) powders are very similar to stoichiometric silicon carbide or silicon nitride. The valence states distributions are significantly different for the two compounds, due essentially to the presence of the lone pair N $2p\pi$ orbital at the top of the VB in silicon nitride. For ternary systems, differences are observed between the VB and CB distributions observed from two LS powders corresponding to C/N values 0.22 and 0.93. They are interpreted in terms of differences in local bonding of Si atoms. In one case, for C/N (atomic ratio)=0.93, both Si-C_4 and Si-N_4 groups associated, respectively, with silicon carbide and silicon nitride compounds are present in the network while for C/N=0.22, the results are consistent with the existence of a local Si environment in which both Si-C and Si-N are present around the same Si atom, as already proposed from previous x-ray-photoelectron and extended x-ray-absorption fine-structure studies of the same samples.

I. INTRODUCTION

In recent years, much interest has been focused on nanophase materials which, due to their small size, can offer improved properties as compared to traditional materials.[1,2] The use of nanocomposite materials containing two or more components, one at least having nanometric dimensions, enlarges considerably the possibilities of applications in various fields.[3,4] It has been reported recently that ceramic nanocomposites obtained from nanometric SiC particles dispersed in an insulating matrix (Al_2O_3 or Si_3N_4) have excellent mechanical and electronical properties.[5] These systems are promising materials in the applications of superplasticity.[6]

The production of nanosize (10–100 nm diam) powders by laser synthesis from gaseous or volatile mixtures has appeared for a few years as a powerful method.[7–10] This method is based on the resonance between the emission of a continuous-wave CO_2 laser at 10.6 μm and the absorption of a gaseous precursor. High-purity and ultrafine Si/C/N powders with various compositions and sizes have been prepared from well-adapted precursors, by varying the synthesis conditions: laser frequency and power, proportions of reactants, and flow rate. More recently, it has been shown that liquid precursors can be used in order to have lower cost products.[11] Moreover, using a tunable CO_2 laser it becomes possible to prepare a wide variety of ceramics including oxides.[12–14] This possibility considerably improves the versatility of the method.

The physical properties of these nanometric powders are strongly correlated to their atomic structure. We recently investigated the chemical bonding and local order in Si, Si/N, Si/C, and Si/C/N nanometric powders prepared by laser synthesis, by using both x-ray-induced photoelectron spectroscopy (XPS) and extended x-ray-absorption fine-structure (EXAFS) analysis.[15] These investigations revealed that, under specific synthesis conditions, Si/C/N powders prepared from a $SiH_4+CH_3NH_2+NH_3$ precursor gas mixture are not a simple mixture of stoichiometric silicon carbide and silicon nitride, but they correspond to a tetrahedral atomic arrangement in which both C and N atoms are bonded to the same central Si atom. Similarly, the existence of mixed configuration for Si atoms was found by other groups for laser-synthesized Si/C/N nanoparticles. Thus, XPS and Auger KLL spectra were interpreted by Giorgi *et al.*[16] by the formation of an intermediate carbonitride nanophase besides Si carbide and Si nitride phases. From NMR studies, Suzuki *et al.*[17] conclude that the local atomic structure of Si/C/N systems changes by introducing nitrogen. At low N content, N atoms are dissolved into a β-SiC lattice and a SiC_3N configuration is suggested; at high N content, Si, SiC, Si_3N_4, and amorphous phases such as $SiCN_3$ are present in the sample.

In order to obtain more information on the atomic arrangement in Si/C/N systems than we have already reported by XPS and EXAFS in Ref. 15, we investigated their valence and conduction states, which are quite sensitive to the bonding configuration. This is the purpose of this paper. Two complementary methods were used. By x-ray induced photoelectron spectroscopy, we obtained for each system the total valence-band (VB) distribution modulated by the photoionization cross sections of each atomic species. By soft-x-ray-emission (XES) and -absorption (XAS) spectroscopies, the valence and conduction states with p symmetry around

TABLE I. Preparation conditions of laser-synthesized samples.

	Si/N	Si/C	Si/C/N (1) (C/N=0.93)[a]	Si/C/N (2) (CN=0.22)[a]
Flow rate (cm^3/min.)	SiH_4 120 NH_3 480	CH_3SiH_3 200	SiH_4 340 CH_3NH_2 200 NH_3 0	280 70 250
S (BET) (m^2/g)	71	34	47	26
Equiv diam (nm)	26	55	40	72

[a]From chemical analysis results (Ref. 9).

Si sites were investigated from the analysis of both Si $K\beta$ ($3p \rightarrow 1s$) emission band and near-edge Si K photoabsorption spectra. As in our previous work,[18] the XPS and x-ray spectra (XES, XAS) were adjusted on a common energy scale referred to the Fermi level. Consequently, our results provide information on the relative position of the Si $3p$ states in the valence-band distribution and on the relative energy position of valence and conduction Si p states. We investigated two laser-synthesized (LS) binary systems Si/C and Si/N and two ternary Si/C/N powders with C/N atomic ratio equal to 0.93 and 0.22. For these samples, information on the local atomic configurations and local order were already obtained from the study of XPS Si $2p$, C $1s$, and N $1s$ core levels and EXAFS spectra.[15] In Sec. II experimental details are briefly described. The experimental XPS and XES-XAS results are presented in Sec. III and discussed comparatively in Sec. IV of this paper.

II. EXPERIMENTS

The samples were prepared by laser pyrolysis of appropriate gaseous precursors in the same conditions as reported previously,[15] summarized in Table I.

XPS VB spectra were obtained by using a Mg $K\alpha$ incident radiation ($h\nu$=1253.6 eV). The electrostatic hemispherical analyzer was used in the fixed analyzer transmission mode with a pass energy equal to 40 eV. Under these conditions, the full width at half maximum (FWHM) of the Ag $3d_{5/2}$ line is 0.8 eV. The XPS VB spectra were scanned with a 0.2-eV step. The samples were pressed pellets prepared from the LS powders. As most of the samples were insulating, a charging effect inducing an energy shift of the peaks was observed. This energy shift remained constant during the acquisition time of the spectra and we calibrate the energy scale by reference to the C $1s$ peak due to the hydrocarbonated contamination present at the surface of the samples. The binding energy (BE) of such a C $1s$ line was fixed at 285.0 eV and the origin of the energy scale corresponds to the Fermi level. A background due to the inelastic electron scattering appears on the experimental spectra shown in the following. The sample thickness involved by the measurements is limited by the electron mean free path Λ, which can be estimated in our experimental conditions to be about 1–3 nm.[19] Considering that 95% of the peak intensity comes from a 3Λ thickness, we estimate the sampled depth to be about 3–9 nm. Consequently, only the superficial part of each powder grain is involved, corresponding to about $\frac{1}{3}$ of the total volume. An oxygen $1s$ peak was observed on the XPS spectra and we estimate the oxide proportion to be a few % only.

The x-ray-emission spectra Si $K\beta$ (Si $3p \rightarrow 1s$) were analyzed with a bent-crystal vacuum spectrometer[20] using as a monochromator either a quartz (1010) crystal ($2d$ =850.766 pm) in the first order of reflection, or a gypsum crystal (020) ($2d$=1519.84 pm) in the second order of reflection bent to a radius of 250 mm. The detector was a proportional counter (500 mb Ar/CH_4 90/10) with an entrance slit fixed at 50 μm. The spectra were scanned with a 0.2-eV-wide step. The total instrumental broadening, mainly due to the monochromator itself, is estimated to be about 0.3 eV.[18] The emissive target was prepared by depositing a thin layer of LS powder onto a copper anode. The spectra were excited by electron bombardment with exciting conditions 5 kV, 5 mA. The thickness sampled is determined by the penetration of the incident electron beam. In our experimental conditions, we estimate the thickness of the emitting layer to be about 0.5 μm. Thus in this case the whole volume of the powder particles is concerned.

The photoabsorption measurements were carried out at Laboratoire pour l'Utilisation du Rayonnement Electromagnétique (Orsay). The Super-ACO storage ring was operating at 1.5 GeV, and the average current was approximately 100 mA. A two-crystal monochromator equipped with InSb (111) crystals ($2d$=748.06 pm) was used. The photoabsorption spectra presented in this paper corresponding to the Si K-edge energy range x-ray-absorption near-edge structure (XANES), that is, 1750–1950 eV, were obtained in the transmission geometry and scanned with a 0.2-eV-wide step. The detector was a proportional counter filled with a 300-mb Ar/CH_4 (90/10) mixture. The absorbing screens were obtained by depositing LS powders onto 5-μm-thick millipore polycarbonate membranes. The spectra of the incident beam were obtained through a membrane without powder. The instrumental resolution is evaluated to be approximately 0.4 eV.[21] The analysis of EXAFS spectra obtained from the same samples was reported previously.[15] As the measurements are achieved by transmission through a screen a few-μm-thick prepared from LS powder, the data concern the whole thickness of the samples, corresponding to several grains.

In order to align the XPS and XES and XAS data on a common energy scale, the Fermi-level position is taken as reference energy in all cases. XPS results are obtained on a BE scale with origin at E_F. XES and XAS spectra are measured as a function of the photon energy; in this energy scale, the Fermi-level position is given by the Si $1s$ binding-energy value. The determination of this energy cannot be directly done by the XPS measurements, performed in our case with Mg $K\alpha$ or Al $K\alpha$ incident beam. We determine Si $1s$ binding energy for each sample by combining XES measurement of Si $K\alpha_1$ line ($2p_{3/2} \rightarrow 1s$) transition energy and XPS measurement of the Si $2p_{3/2}$ core level, as previously done.[18]

III. EXPERIMENTAL RESULTS

A. XPS results

The Si $2p$, C $1s$, and N $1s$ core levels from Si-C, Si-N, and Si-C-N (1) and (2) LS powders have been already reported and discussed in detail.[15] From these measurements,

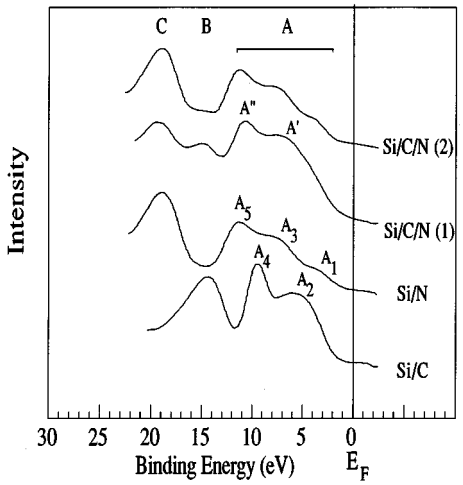

FIG. 1. XPS valence-band spectra of laser-synthesized Si/C, Si/N, Si/C/N (1) and Si/C/N (2) samples

we evaluated the proportion of the superficial SiO_2 layer at about 11–17% of the main contribution.

The VB spectra of LS powders Si/C, Si/N, Si/C/N (1) and (2) are plotted in Fig. 1 in the binding-energy range 0–22 eV, with E_F as origin. Let us note that the O $2s$ contribution, principally due to SiO_2 is located at higher BE (around 25 eV). Taking into account the relative intensity of the O $2s$ peak, we estimate that the contribution of silicon oxide in the 0–22 eV range is negligible. The intensity distributions, normalized in amplitude, are significantly different for the four samples. The spectra exhibit a broad band A which extends between 0 and about 13 eV followed by peaks B and C, at about 15 and 19 eV, respectively, which have different relative intensities in the samples considered. The distances from these features to E_F are given in Table II.

The Si/C VB spectrum is almost identical to a β-SiC spectrum, as already reported.[22] Part A exhibits two peaks labeled A_2 and A_4 located at 5.7 eV and 9.5 eV, respectively. From a comparison with theoretical densities of states[23] these peaks are attributed to C $2p$ states mixed with Si $3p$ and Si $3s$, respectively; a wide minimum separates A_4 from peak B, located at 14.4 eV BE, which corresponds to C $2s$ states mixed to Si $3p$ and Si $3s$.

The Si/N spectrum is very similar to the silicon nitride (Johnson Mattey, 99.99% powder) XPS VB spectrum previously reported.[24] The upper part A exhibits three structures labeled A_1, A_3, and A_5 located at 3.3, 7.5, and 11.4 eV, respectively. From the previous study of Si_3N_4 XPS and XES spectra,[24] in agreement with theoretical density of states (DOS),[25] peak A_1 is unambiguously attributed to a N $2p\pi$ lone pair, peaks A_3 and A_5 are associated, respectively, with N $2p$–Si $3p$ states and N $2p$–Si $3s$ states. Peak C, well separated from the A band, is due to N $2s$ states mixed to Si $3s$–Si $3p$ states.

TABLE II. Energy positions of the XPS VB features (eV).

	A_1	A_2	A'	A_3	A_4	A''	A_5	B	C
Si/C		5.7			9.5			14.4	
Si/N	3.3			7.5			11.4		18.9
Si/C/N (1)			7.0			10.8		14.9	19.3
Si/C/N (2)	3.9			7.6			11.4		19.0

The VB spectra from Si/C/N (1) and (2) are quite different in shape.[26] The spectrum from sample 1 with C/N=0.93 exhibits only two structures A' and A'' at 7.0 and 10.8 eV. The energy position of A' is intermediate between that of A_2 from Si/C and A_3 from Si/N. Similarly, A'' is located between A_4 (Si/C) and A_5 (Si/N) (see Table II). The low BE edge of the spectrum is more contrasted than in the Si/N spectrum; however it is less abrupt than in Si/C. It is noteworthy that both peaks B and C are observed in this spectrum at 14.9 and 19.3 eV. Their energy positions correspond to those of peaks B from Si/C and C from Si/N, suggesting that both C $2s$ and N $2s$ mixed to Si $3s$,$3p$ states are present.

For Si/C/N (2), which corresponds to C/N=0.22, the spectrum is rather similar to the Si/N one. The upper band A exhibits three structures (see Table II); it is followed by a sharp peak C located at 19.0 eV, well separated from band A; consequently, the VB states correspond essentially to those of Si/N bonds found in silicon nitride. Let us note that the minimum between A and C is not so marked as in the Si-N spectrum and that a shoulder is clearly observed around 15 eV.

B. XES and XAS results

In Figs. 2–5 we have plotted, in the same BE scale with E_F as origin, the XES Si $K\beta$, the XPS valence band, and the XANES spectra for LS powders Si/C, Si/N, and Si/C/N (1) and (2). Let us recall that the XES Si $K\beta$ curves give the Si $3p$ valence-band states distribution and the XANES curves the unoccupied Si p states distribution.

Si $K\beta$ from Si/C LS powder is very similar to the silicon carbide Si $K\beta$ spectrum observed previously.[22,27] The maximum intensity located at 5.3 eV from E_F corresponds to peak A_2 of the XPS VB spectrum, the decrease of intensity towards E_F is rather abrupt; its inflection point coincides with that of the low BE edge of XPS VB spectrum. The high BE edge is less steep and shows a shoulder at about half maximum; that is, at an energy corresponding approximately to the energy of peak A_4. Finally a small intensity peak, well resolved from the main band, is observed at 15 eV from E_F, showing that Si $3p$ states are present deeper in the VB. This small peak coincides with peak B of the XPS VB spectrum. The XAS spectrum of Si/C presents a two-step edge extending from about 0 to 5.3 eV, where a sharp maximum occurs. A secondary maximum occurs at 11.5–12 eV and a strong peak at 19 eV from E_F.

Si $K\beta$ from Si/N (Fig. 3) is a quasisymmetric band; its overall shape is close to that of the silicon nitride $K\beta$ emission band previously reported;[24] however, its FWHM is wider, 6.5 instead of 5.5 eV. The energy position of the maximum, 8.4 eV from E_F, gives the mean BE of the Si $3p$ states; it is the same as in the nitride. This maximum coincides approximately with peak A_3 of the XPS VB spectrum. Consequently, this result confirms that the peak A_1 of the XPS VB spectrum corresponds to pure nitrogen states. We note that the decrease of intensity on the low BE tail of Si $K\beta$ is not steep but exhibits some tailing; we attribute this effect to the presence of a few Si-Si bonds in this sample. Let us recall that these like-atom bonds had already been re-

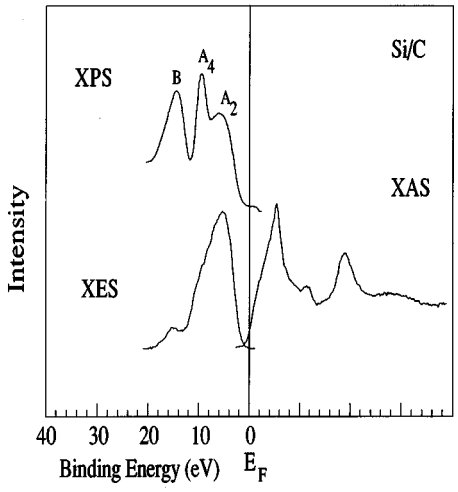

FIG. 2. XPS VB, XES, and XAS spectra from Si/C adjusted in a common energy scale with E_F as origin.

vealed by the study of the Si $2p$ core level from the same sample.[15] The low-intensity peak located at 19.5 eV corresponds to peak C of the XPS VB spectrum and reflects the presence of Si $3p$ states mixed to N $2s$ ones in this part of the valence band. The XAS spectrum of Si/N consists of a steep edge whose inflection point is located 1 eV above E_F, followed by a maximum at 3.8 eV from E_F. A second maximum is observed around 22 eV from E_F.

In Si/C/N (1) and (2), the Si $K\beta$ emission band is a quasisymmetric band with FWHM 7.7 and 6.5 eV, respectively (Figs. 4 and 5).[26] In sample 1, the main peak is accompanied by a shoulder at 8.5 eV, in coincidence with the Si/N $K\beta$ maximum; a faint feature around 5 eV could be a signature of the Si/C Si $K\beta$ maximum. The distance from E_F of the low BE edge, measured at half amplitude, is about the same as in Si/C. The Si $K\beta$ spectrum is broader than in binary compounds and can be considered approximately as a sum of both the Si/C and the Si/N spectral distributions. It is noteworthy that, in the high BE range, a small feature is observed at the energy positions of B. The photoabsorption edge of Si/C/N (1) has a continuous slope, slightly less abrupt than in Si/N spectrum. Beyond the first maximum, two peaks are observed at about 3.8 and 5.3 eV from E_F, that is, at approximately the same position as in Si/C and Si/N photoabsorption curves, respectively. Beyond this energy range, a slight feature is noted at 11.5 eV from E_F and a strong maximum at 19.5 eV from E_F.

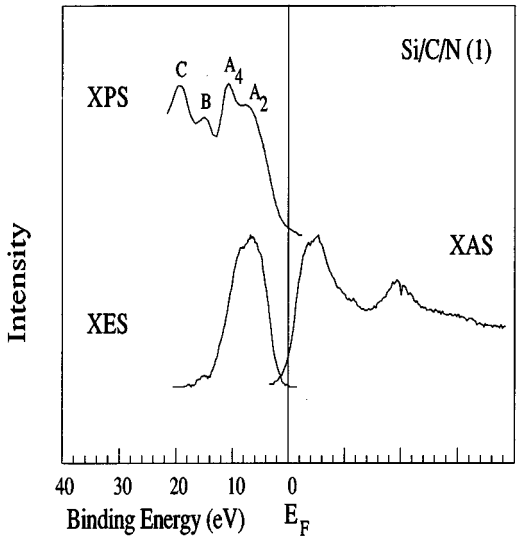

FIG. 4. XPS VB, XES, and XAS spectra from Si/C/N (1) adjusted in a common energy scale with E_F as origin.

In Si/C/N (2), the Si $K\beta$ spectrum is narrower than in Si/C/N (1); its shape is rather similar to Si/N Si $K\beta$. The maximum corresponds approximately to peak A_3 of the XPS VB curve, while no feature appears at the energy position of A_1. The photoabsorption curve exhibits a strong maximum at 3.6 eV from E_F, i.e., close to that observed in Si/N photoabsorption, giving the appearance of a ''white line.'' A shoulder is observed at 7 eV and a wide maximum at 21 eV from E_F.

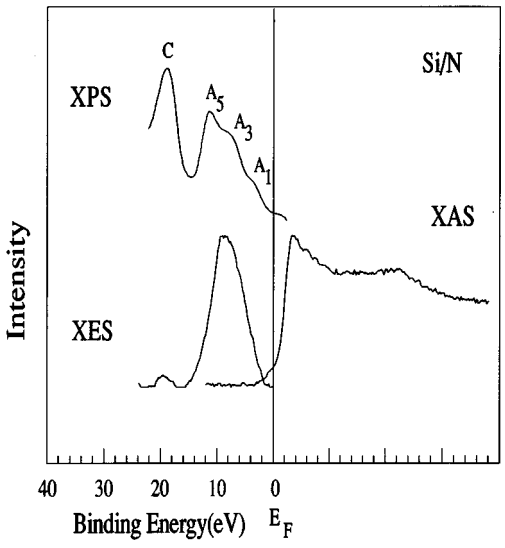

FIG. 3. XPS VB, XES, and XAS spectra from Si/N adjusted in a common energy scale with E_F as origin.

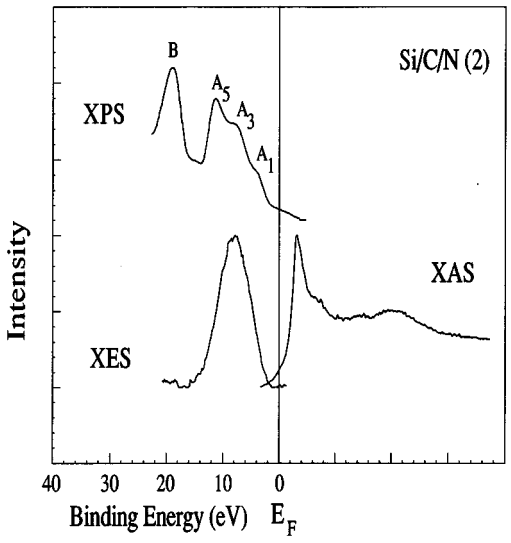

FIG. 5. XPS VB, XES, and XAS spectra from Si/C/N (2) adjusted in a common energy scale with E_F as origin.

TABLE III. Photoionization cross sections in barns/atom, from Ref. 28 ($h\nu$=1253.6 eV).

C 2s	C 2p	N 2s	N 2p	Si 3s	Si 3p
1.04×10^{3}	4.1×10^{1}	1.86×10^{3}	2.19×10^{2}	1.61×10^{3}	3.31×10^{2}

IV. DISCUSSION

Complementary information on the valence and conduction bands is obtained from the study of both XPS and XES-XAS data. XPS spectra correspond to the total valence distribution modulated by the photoionization cross sections which, in our case, emphasizes s states as compared to p states; atomic photoionization cross sections for $h\nu$=1253.6 eV, calculated by Ref. 28, are given in Table III.

XES and XAS spectra correspond in first approximation to the convolution of the Si p occupied or unoccupied states distributions by the Lorentzian distribution of the Si 1s core-level distribution, which is about 0.5 eV wide.[24] Let us recall that XPS measurements concern a sampled thickness of a few nm from the surface of the sample. As a consequence, in the case of LS powders studied in this work, the measurement concerns only a superficial layer of each grain. In contrast, XES and XAS involve a thickness equivalent to several grains of the powder, so the total volume of each powder grain is involved.

For binary systems Si/C and Si/N, the experimental XPS and XES-XAS spectral curves are qualitatively well reproduced by the DOS calculations performed by Robertson in the tight-binding formalism for crystalline β-SiC[23] and α-Si_3N_4 crystalline phases.[25] Differences in relative intensities of the peaks are due to differences in photoionization cross sections (see Table III). These conclusions are in total agreement with those obtained for the same sample from the XPS core levels and EXAFS studies.[15]

In Si/C, our results confirm unambiguously the existence in the LS material of a chemically ordered sp^3 bonded network with Si-C heteropolar bonds. The Si 3p states whose position corresponds to Si $K\beta$ emission are mainly located at the top of the valence band, in coincidence with peak A_2 of XPS. The sharp XPS peak A_4 at 9.5 eV, at the same energy as a low feature of Si $K\beta$, can be associated with sp states. From Robertson calculations, we have deduced that this peak is due to mixed Si 3s and C 2p states; from our results Si 3p states are also involved in this energy range. A sharp minimum, corresponding to the ionicity gap, separates the maximum A_4 from peak B; this energy gap is characteristic of Si-C bonds in a crystalline network. The minimum is expected to be partially filled in the case of amorphous SiC as predicted from a theoretical study of a-SiC density of states performed by Finocchi *et al.*[29] Peak B is largely C 2s in character, with a small, but nonnegligible Si 3p contribution as clearly revealed by our XES data, in excellent agreement with theoretical predictions. As concerns the conduction band, an overall agreement is found between the photoabsorption curve and the theoretical DOS for which the absorption edge is followed by two peaks attributed to antibonding Si 3p–C 2s and Si 3p C 2p states distant by about 3 eV; the nonresolution of these features in the experimental curve is probably due to the core-level broadening. Beyond the first peak, the experimental photoabsorption curve shows well-resolved peaks that reveal the existence of a well-organized network. This is in agreement with the EXAFS results we have obtained for this LS powder, which clearly revealed the existence of Si-C_4 groups.

The influence of hydrogen incorporation in a SiC matrix has been recently studied in a theoretical simulation.[30] For a-SiC:H alloys at stoichiometric composition, containing 20% hydrogen, these authors predict that hydrogen atoms are bonded to both carbon and silicon atoms and that the presence of hydrogen favors the formation of a tetrahedral network and thus enhances the chemical order in the material. This is well supported by our results.

In Si/N powder, the VB distribution observed experimentally is very close to the Si_3N_4 one. Our results confirm that the top of the VB corresponds to a N 2$p\pi$ lone pair orbital, in agreement with theoretical results.[25] The lone pair orbital is characteristic of the planar configuration of N atoms surrounded by three silicon atoms. This feature is followed by mixed Si 3p–N 2p and Si 3s–N 2p states; N 2s states mixed to Si 3s-3p states appear as a well-resolved peak. A broadening of the Si 3p distribution when going from Si_3N_4[24] to Si/N powders is noted. Two effects can contribute to this broadening. The first effect is due to a loss of long-range order as compared to well-crystallized silicon nitride; a topological disorder attributed to fluctuation of bond lengths and bond angles has been evidenced in this material from a previous study.[15] Let us note that this effect does not modify the overall shape of the VB distribution, which is essentially determined by the short-range order.[31] The second effect is the presence of like-atoms bonds Si-Si in a low but not negligible proportion as already revealed by the Si 2p core-level study.[15] Thus LS Si/N powders are characterized by both structural and chemical disorder. The presence of hydrogen in the network is possible, according to the preparation conditions. In a previous study of a-SiN_x:H alloys, we had shown that hydrogen atoms are in this case preferentially bonded to nitrogen atoms.[31] In this case, the Si states distribution should not be significantly modified. From the results obtained by Ley for hydrogenated a-Si-N_x samples[31] hydrogen incorporation involves a recession of the VB maximum, which remains probably small for the low H concentration corresponding to our samples. Moreover, due to the low value of the H 1s cross section under our experimental conditions ($h\nu$=1253.6 eV), the effect of hydrogen on the XPS valence-band spectrum remains probably quite negligible.

The first photoabsorption peak gives the distribution of the unoccupied Si p states; its shape corresponds to a disordered network and supports the previous EXAFS results on the same samples. In this energy range, the DOS calculations for silicon nitride,[25] which covers an energy range of about 12 eV from E_F, predicts the existence of a broad maximum between 5 and 10 eV from E_F; the shift between the experimental and the calculated data that we have already mentioned[15] can be explained by the experimental gap value introduced in the calculation.

It is interesting to note that the presence of hydrogen in the network favors a higher chemical and structural order in the case of Si/C systems; on the contrary, it involves a tendency to more disorder in the case of Si/N powder; in both cases the laser power used for the synthesis is 600 W.

In Si/C/N powders, the valence- and conduction-band dis-

tributions are quite different according to the composition. For the C/N value equal to 0.93 [Si/C/N (1))], our results indicate clearly that Si atoms are involved in both carbide and nitride configurations. This is evidenced from the XPS VB spectrum, which reveals that both C $2s$ and N $2s$ states, mixed to Si sp states, are present; on the XES Si $K\beta$ spectrum, we observe a small peak at the energy position of B (Si $3p-$C $2s$ states). Moreover, these results are well supported by the photoabsorption spectrum of Si/C/N (1), which shows two features close to the edge, corresponding to the first absorption maximum of Si/N and Si/C, respectively; the next features being close to those observed in the Si/C spectrum.

In Si/C/N (2) with C/N=0.22, the spectral distributions are rather close to those of Si/N, but slight differences are noted which clearly indicate that the network is not identical to silicon nitride:

(i) The XES Si $K\beta$ spectrum (Fig. 5) shows that the Si $3p$ maximum is slightly shifted towards low BE as compared to Si/N Si $3p$, without broadening; this result shows that additional Si-C bonds are present in the network, a few Si-N bonds being replaced by Si-C bonds.

(ii) The minimum between A_5 and B on the XPS VB spectrum is slightly enhanced as compared to that of Si/N. The energy position of this minimum corresponds to that of peak B of the Si/C spectrum and, consequently, this additional shoulder reveals that C $2s$ states due to a few Si-C bonds are present in the network.

On the photoabsorption curve, the sharp maximum following the photoabsorption edge corresponds to the Si/N first maximum; it is characteristic of a crystalline Si_3N_4 network. A maximum is located at about 20 eV, close to both Si/N and Si/C maxima. The presence of a shoulder at about 7 eV from E_F could result from Si-C bonds.

Consequently, for sample Si/C/N (2), our experimental results are consistent with the existence of a single type of chemical environment of Si atoms with both Si-N and a few Si-C bonds in the network. This is in quite good agreement with our previous results obtained for the same samples from XPS core levels and EXAFS studies.[15]

Therefore, our results reveal that the local environment of Si atoms depends essentially on the preparation conditions of the powder. For C/N ratio close to 1, Si atoms are involved in both Si-C_4 and Si-N_4 configurations. EXAFS data for these samples[15] indicated that atomic distances Si-C and Si-N are close to the corresponding crystalline values. Moreover, they clearly revealed the presence of βSiC microcrystallites in the material; we suggested that the microcrystals could be contained in an amorphous phase of SiN_4 units, H atoms being present in NH_x, CH_x, or SiH_x groups. The present results on valence and conduction states of the material support quite well the preliminary results.

For an initial ratio C/N equal to 0.22, we confirm that most Si atoms are bonded to both C and N atoms. The shape of the Si $2p$ line suggests a single type of Si environment as discussed in Ref. 15. This is confirmed by the shape and width of Si $3p$ distribution observed in the present work. Thus in this case a type of atomic arrangement is obtained that is of great interest for possible future applications.

V. CONCLUSION

We have analyzed the electronic structure of laser-synthesized Si/C, Si/N, and two Si/C/N samples by using two complementary methods. By x-ray-photoelectron spectroscopy, we determined the total valence-band distribution. By soft-x-ray-emission and -absorption spectroscopies, we have obtained the partial Si $3p$ valence-band and Si p conduction-band states.

For binary systems Si/C and Si/N, the spectral distributions are similar to those observed previously for stoichiometric phases β-SiC and α-Si_3N_4. The results are discussed in relation to density-of-states calculations. For SiC, the Si $3p$ states mixed to C $2p$ states are located at the top of the VB, followed by Si $3sp$ and Si $3s$ states mixed to C $2p$ states. A well-separated peak is located at 14.4 eV from E_F and attributed to the contribution of C $2s$ states mixed to Si $3s$ and $3p$ states. For the Si/N LS system, a N $2p$ lone pair orbital characteristic of planar configuration of N atoms surrounded by three Si atoms present in silicon nitride is identified. It is followed by mixed Si $3p-$N $2p$ and Si $3s-$N $2p$. Mixed N $2s-$Si $3s,3p$ states are identified at 18.9 eV from E_F. The overall broadening of the VB distribution observed in Si/N powder as compared to the Si_3N_4 stoichiometric phase is interpreted by both structural and chemical disorder in LS material.

In ternary systems, the valence and conduction states distributions are strongly dependent on the C/N concentration ratio. For C/N=0.93, Si atoms are clearly involved in both silicon carbide and silicon nitride configurations; this result is unambiguously evidenced by the existence of both peaks B and C in the XPS spectrum of these powders. On the other hand, for C/N=0.22, a local atomic arrangement with both C and N atoms surrounding the same Si atom is suggested by the experimental results, in agreement with previous XPS core levels and EXAFS results. These results are quite promising for possible applications of the laser-synthesized powders. Further investigations are in progress for nanometric Si/C/N powders prepared from appropriate aerosol precursors.

[1] R. W. Siegel, in *Nanophase Materials: Synthesis, Structure and Properties*, edited by F. E. Fujita, Springer Series in Materials Science–Physics of New Materials Vol. 27 (Springer-Verlag, Berlin, 1994), p. 65.

[2] R. Dagani, Chem. Eng. News **23**, 18 (1992).

[3] S. Komarneni, J. Mater. Chem. **2**, 1219 (1992).

[4] M. Suzuki, Y. Maniette, Y. Nakata, and T. Okutani, J. Am. Ceram. Soc. **76**, 1195 (1993).

[5] A. Sawasuchi and K. Toda, J. Am. Ceram. Soc. **74**, 1142 (1991).

[6] F. Wakai, Y. Kodama, S. Sakaguchi, N. Murayama, K. Izaki, and K. Niihara, Nature **344**, 421 (1990).

[7] J. S. Haggerty and R. W. Cannon, in *Laser Induced Chemical*

Processes, edited by J. I. Steinfeld (Plenum, New York, 1981), Chap. 3.
[8] M. Cauchetier, O. Croix, and M. Luce, Adv. Ceram. Mater. **3**, 548 (1988).
[9] M. Luce, O. Croix, C. Robert, and M. Cauchetier, in *Ceramic Powder Science III*, edited by G. L. Messing, S. I. Hirano, and H. Hausner (American Ceramic Society, Westerville, 1990), Chap. 12, p. 548.
[10] M. Cauchetier, O. Croix, M. Luce, M. I. Baraton, T. Merle, and P. Quintard, J. Eur. Ceram. Soc. **8**, 215 (1991).
[11] M. Cauchetier, O. Croix, N. Herlin, and M. Luce, J. Am. Ceram. Soc. **77**, 993 (1994).
[12] M. Cauchetier, N. Herlin, E. Musset, M. Luce, H. Roulet, G. Dufour, A. Gheorghiu, and C Sénémaud (unpublished).
[13] J. D. Casey and J. S. Haggerty, J. Mater. Sci. **22**, 4307 (1987).
[14] E. Borsella, S. Botti, R. Giorgi, S. Martelli, S. Turtu, and G. Zappa, Appl. Phys. Lett. **63**, 1345 (1993).
[15] A. Gheorghiu, C. Sénémaud, H. Roulet, G. Dufour, T. Moréno, S. Bodeur, C. Reynaud, M. Cauchetier, and M. Luce, J. Appl. Phys. **71**, 4118 (1992).
[16] R. Giorgi, S. Martelli, S. Turtu, E. Borsella, and S. Botti, Surf. Interface Anal. **22**, 248 (1994).
[17] M. Suzuki, Y. Hasegawa, M. Aizawa, Y. Nakata, T. Okutani, and K. Uosaki, J. Am. Ceram. Soc. **78**, 83 (1995).
[18] C. Sénémaud and I. Ardelean, J. Phys. Condens. Matter. **2**, 8741 (1990).
[19] M. P. Seah and W. A. Dench, Surf. Interface Anal. **1**, 1 (1979).
[20] C. Sénémaud, D. Laporte, J. M. André, R. Khérouf, P. Paquier, and M. Ringuenet (unpublished).
[21] E. Bouisset, J. M. Esteva, R. C. Karnatak, J. P. Connerade, A. M. Flank, and P. Lagarde, J. Phys. B **24**, 1609 (1991).
[22] M. Driss-Khodja, G. Dufour, A. Gheorghiu, H. Roulet, C. Sénémaud, M. Cauchetier, O. Croix, and M. Luce, Mater. Sci. Eng. B **11**, 97 (1992).
[23] J. Robertson, Philos. Mag. B **66**, 615 (1992).
[24] C. Sénémaud, M. Driss-Khodja, A. Gheorghiu, S. Harel, G. Dufour, and H. Roulet, J. Appl. Phys. **74**, 5042 (1993).
[25] J. Robertson, Philos. Mag. B **63**, 47 (1991).
[26] M. Driss-Khodja, thèse de l'Université Pierre et Marie Curie, Paris, 1994.
[27] W. Zahorowski, G. Wiech, H. Mell, and G. Weiser, J. Phys. Condens. Matter, **1**, 9571 (1989).
[28] I. M. Band, Y. I. Kharitonov, and M. B. Trzhaskovskaya, At. Data Nucl. Data Tables **23**, 443 (1979).
[29] F. Finocchi, G. Gallia, M. Parrinello, and C. M. Bertoni, Physica B **85**, 379 (1993).
[30] F. Finocchi and G. Galli, Phys. Rev. B **50**, 7393 (1994).
[31] R. Kärcher, L. Ley, and R. L. Johnson, Phys. Rev. B **30**, 1896 (1984).
[32] M. Driss-Khodja, A. Le Corre, C. Sénémaud, A. Gheorghiu, M. L. Thèye, B. Allain, and J. Perrin, J. Non-Cryst. Solids, **114**, 498 (1989).